Click Here for Full Article

Intermittent multidecadal-to-centennial fluctuations dominate global temperature evolution over the last millennium

Davide Zanchettin,[1] Angelo Rubino,[2] and Johann H. Jungclaus[1]

Received 22 April 2010; revised 27 May 2010; accepted 8 June 2010; published 22 July 2010.

[1] Observed climate time series covering several centuries are often characterized by fluctuations on multidecadal-to-centennial timescales. These are not homogeneously distributed in time: Instead, they appear within irregularly intermittent temporal intervals, whose irregular duration varies, in general, with the signal fluctuation frequency. A similar irregularly intermittent, frequency-dependent appearance of energetic fluctuations is found in long-term Earth system model integrations, consisting of a multi-millennia control experiment (i.e., an unforced simulation) and forced simulations covering the last millennium. Here, for the first time, we investigate the long-term relative importance of internal and externally-driven variability and their possible interferences on Global Surface Temperature (GST). Multidecadal GST fluctuations are mostly associated to internal variability. Externally-forced perturbations acting predominantly on centennial timescales tend to overwhelm such variability and to enhance O(~200 years) GST fluctuations. Externally-forced perturbations tend also to correspond to major changes in the coherency among internal climate processes, and among them and GST. **Citation:** Zanchettin, D., A. Rubino, and J. H. Jungclaus (2010), Intermittent multidecadal-to-centennial fluctuations dominate global temperature evolution over the last millennium, *Geophys. Res. Lett.*, *37*, L14702, doi:10.1029/2010GL043717.

1. Introduction

[2] Millennium-scale numerical global climate simulations like those performed in the framework of the "Community Simulation of the Last Millennium" (hereafter: CSLM) [*Jungclaus et al.*, 2010] offer a valuable opportunity to understand details of multidecadal and larger timescales climate variability. In particular, such simulations have been used to produce temperature time series resembling those reconstructed for known climatic eras such as the "Medieval Warm Period" and the "Little Ice Age" [*Shindell et al.*, 2001; *Crespin et al.*, 2009; *Trouet et al.*, 2009], to assess the interplay between internal and forced variability and trends [*Shindell and Schmidt*, 2003; *Goosse et al.*, 2005; *Pongratz et al.*, 2009], and to put the simulated anthropogenic contribution to climate change in the context of long term climate variability [*Gerber et al.*, 2003]. Less attention, however, has been devoted at studying intrinsic characteristics of simulated multidecadal-to-centennial fluctuations like periods and intensity of their appearances and at envisaging possible links of such variability to internal variability and/or external forcing. Nonetheless, an assessment and a deep understanding of simulated mode excitability and its possible triggering mechanisms may constitute a prerequisite to correctly interpret simulated long-term climate variability and, hence, to properly relate simulations and observations. Also, the interplay among different long-term variability patterns influences crucially climate predictability, including that at decadal and multidecadal timescales.

[3] One of the longest time series of climate observations is the monthly Central England Temperature (CET) record [*Parker et al.*, 1992], see auxiliary material.[3] Once deseasoned, the spectral density profile and the corresponding wavelet spectrum of this time series (Figure 1, top) exhibit its strongest fluctuations for periods around and above the decadal timescale, with a clear peak around 70 years (which explains about one third of the total variability at decadal and longer timescales). Such an evolution dominated by multidecadal-to-centennial periodicities is a common feature characterizing also other long climate time series, such as many of the longest series of temperature observations [*Lawson et al.*, 1981; *Polyakov et al.*, 2005; *Zhang et al.*, 2007]. Similarly, global temperature estimates based on instrumental records covering the last ~160 years show a strong centennial trend explaining up to 2/3 of the total variability, while fluctuations around the bidecadal and the O(50 years) bands dominate the residual variability (Figure S1a).

[4] A glance at the temporal structure of CET variability sheds light on characteristics of its frequency peaks, which correspond to frequently observed climate peculiarities as well: Signals below and around the decadal band appear only very sporadically as patches of rather concentrated episodes. Though still intermittent, multidecadal signals, instead, seem to exist more continuously. We note also the existence of irregularly alternating, prolonged periods during which multidecadal fluctuations are/are not significant contributions to the observed variability. The limited temporal domain of the available instrumental-based estimates for the global temperature bounds our capability of inferring the robustness through time of the observed multidecadal and centennial timescale fluctuations. Nonetheless, irregularly alternating multidecadal and centennial fluctuations of climate variability can be commonly detected in other long observed climate series (Figure S1b).

[5] However, such characteristics are not exclusively encountered in instrumental records, as they also appear in reconstructed time series based on climate proxies. For instance, the recent reconstruction of low-latitude North

[1]Ocean in the Earth System Department, Max-Planck-Institute for Meteorology, Hamburg, Germany.
[2]Department of Environmental Sciences, University of Venice, Venice, Italy.

Copyright 2010 by the American Geophysical Union.
0094-8276/10/2010GL043717

[3]Auxiliary materials are available in the HTML. doi:10.1029/2010GL043717.

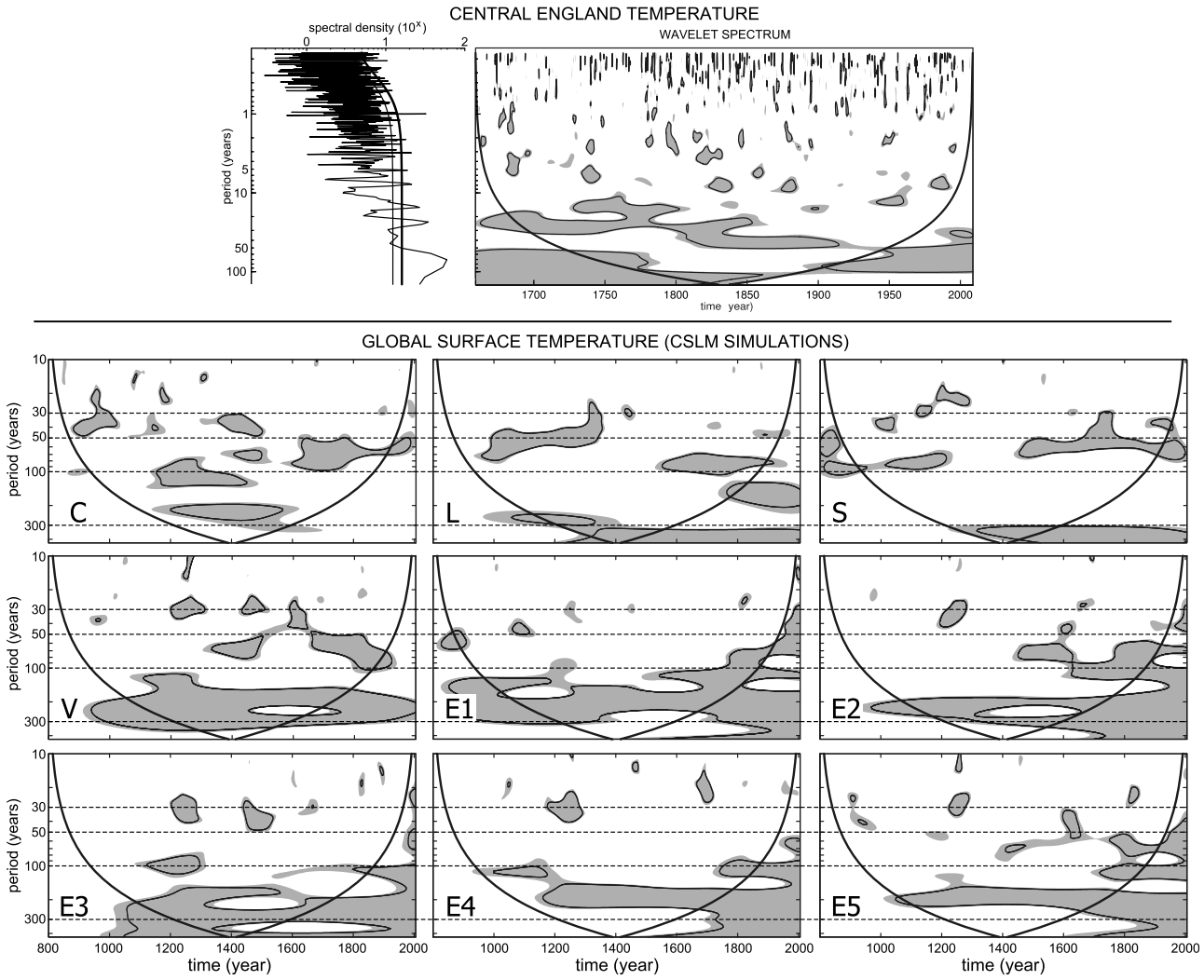

Figure 1. (top left) Power spectrum and (top right) wavelet spectrum of 1659–2008 monthly temperatures for the Central England region (CET). (bottom) Wavelet spectra of the annual Global Surface Temperature (GST) estimates for the period AD 800–2005 evaluated by the nine CSLM simulations detailed in Table 1 (the symbol on the bottom left corner of each plot identifies the simulation). Lines (grey shading) individuate periodic signals which are statistically significant at 95% (90%) confidence. Thick lines in the wavelet spectra individuate the cone of influence, where border effects occur.

Atlantic Sea Surface Temperatures (SST) since 1552 [*Saenger et al.*, 2009] indicates significant near-decadal fluctuations throughout the centuries but only rather evanescent significant multidecadal variations. Therefore: Are numerical climate models able to reproduce these frequently detected features of climate variability on a global scale? And, if so: What can we learn about fundamental processes involved in such signal generation and propagation? To answer these questions we investigate the results of eight 1200-year long simulations over historical times and a 3100-year long control experiment conducted within the CLSM project using the Earth System Model (ESM) developed at the Max Planck Institute for Meteorology.

2. Model Description and Experimental Setup

[6] The ESM consists of a general circulation atmospheric model (ECHAM5 [*Roeckner et al.*, 2003]) coupled with a general circulation oceanic model (MPI-OM [*Jungclaus et al.*, 2006]) with a full carbon cycle implementation (see auxiliary material for details). Forced experiments apply state-of-the-art reconstructions of natural forcing (volcanic aerosols and Total Solar Irradiance or TSI) and anthropogenic forcing (land-cover changes, greenhouse gas emission) for the period AD 800–2005. Table 1 gives an overview over the ESM experiments analyzed in this study.

[7] As a reference variable for our investigation we use the annual-average Global Surface Temperature (GST), whose basic statistics for the nine simulations are summarized in Table 1. We also investigate the simulated behavior of different climate indices, namely the Pacific Decadal Oscillation (PDO), the Atlantic Multidecadal Oscillation (AMO), and the Arctic Oscillation (AO). We also make use of a Meridional Overturning Circulation (MOC) index, which is defined as the annual zonally-averaged overturning

Table 1. Characteristics of the Nine CLSM Simulations Used in This Study and Standard Deviations[a]

Simulation	Forcing	Time Span	σ_{GST} (K)	$\sigma_{GST,O(50)}$ (K)	$\sigma_{MOC,O(50)}$ (Sv)
C	Control run (unperturbed climate)	AD 800-3900	0.202	0.042	0.376
L	Land-use change forcing only	AD 800-2005	0.207 0.202[b]	0.058 0.040[b]	0.342
S	Solar forcing only	AD 800-2005	0.206	0.044	0.376
V	Volcanic forcing only	AD 800-2000	0.216	0.071	0.440
E1-E5	All-forcing, different initial ocean conditions	AD 800-2005	0.235 ± 0.003 0.229 ± 0.003[b]	0.075 ± 0.006 0.072 ± 0.007[b]	0.603 ± 0.103 0.410 ± 0.101[b]

[a]Standard deviations (σ) for: annual-average Global Surface Temperature (GST), multidecadal GST (O(50 years), see auxiliary material) and multidecadal Atlantic Meridional Overturning Circulation (MOC).
[b]Pre-industrial period only (before AD 1850).

transport in the Atlantic Ocean at 30°N and 1000 m depth. The reader is referred to auxiliary material for further details.

3. Results and Discussion

[8] Figure 1 (bottom) illustrates the wavelet spectra of annual GST for the nine CSLM simulations. Beside differences emerging among the exact frequencies of the simulated fluctuations and/or among their exact temporal occurrences, all simulated GST signals show similar, irregularly recurrent manifestations of multidecadal fluctuations, preferably above O(50 years), and a very energetic presence of significant centennial or longer fluctuations. Spectral analysis performed on the annual GST time series for the nine model runs (Figure S2) reveals that, like in the case of the long observed climate signals discussed above, multidecadal (O(50–90 years)) and even longer oscillations exert large contributions to the simulated variability. Indeed, the variance at decadal and longer timescales they explain ranges from 7% to 25% for multidecadal oscillations, and from 7% to 29% for centennial (O(100–300 years)) oscillations. We note that strong irregularly recurrent multidecadal fluctuations appear frequently in simulation C, i.e., they are originated by internal processes alone. Multidecadal fluctuations are also significant contributors to GST variability in simulations L and S, but not in simulations V and E1-E5. In such simulations, the variability is in general larger than in simulation C (see Table 1) and it seems to be dominated by centennial or even longer fluctuations, i.e., external forcings induce centennial GST variability which adds up to internal variability and even overwhelms it. Notably, the energy associated to multidecadal signals in simulation C appears to be almost preserved in simulations V and E1-E5 (Figure S2), i.e., external forcings do not dampen internal variability. To better understand characteristics of GST variability, in particular the nature of interactions between internal multidecadal and externally-forced centennial fluctuations, we analyze the full length (3100 years) of simulation C in more detail. The corresponding wavelet spectrum (Figure 2a) unveils that long periods (several centuries) can emerge, that are not characterized by the presence of any significant manifestation of multidecadal-to-centennial periodicities in GST.

[9] It is beyond the scope of this paper to discuss in all details the mechanisms behind the GST variations in an unperturbed climate system. Here we concentrate our discussion on how several specific atmospheric and oceanic processes, and some known interactions among them, may contribute to the detected non-stationarity in multidecadal-to-centennial internal climate variability. Figures 2b–2d illustrate the wavelet spectra of a selection of prominent climate descriptors: Figure 2b refers to the winter AO, which describes the leading mode of winter variability in the Northern Hemispheric troposphere and is also associated to stratospheric polar variability [*Thompson and Wallace*, 1998], Figure 2c refers to the winter PDO, which describes large-scale SST variability in the extra-tropical North Pacific [*Mantua et al.*, 1997], Figure 2d refers to the Atlantic MOC, which describes the strength of the oceanic thermohaline circulation and, at this latitude, measures the oceanic meridional heat transport. As a typical atmospheric process, the AO displays only sporadic appearance of significant fluctuations above the decadal band. The PDO, instead, shows strong fluctuations at O(50 years) to O(100 years) timescales. We conclude that in an undisturbed simulation, regional SST variability is preferably excited in the low-frequency portion of the multidecadal band. Notably, these periodicities emerge in the spectrum of the simulated Atlantic Multidecadal Oscillation (AMO) as well (Figure S3). Strong fluctuations around O(50 years) to O(100 years) emerge also in the AO spectrum, but they are there mostly confined in the earliest centuries of the run. Possibly, this highlights that non-stationary ocean-atmosphere coupling can intermittently favor/hamper the emergence of multidecadal signals in the hemispheric atmospheric circulation. The MOC exhibits robust, strong variability at timescales longer than O(100 years) and further shows intermittent variability at O(50 years): Deep oceanic processes emerge therefore as key phenomena to interpret simulated long-term climate variability, including multidecadal and even longer (e.g., O(200 years)) GST variability. We note anyway that fluctuations around O(500 years) strongly characterizing the MOC do not emerge in GST (Figure 2a).

[10] Overall, we diagnose a strong linkage of multidecadal GST signals over the full-length of simulation C with the PDO ($r_{O(50)} = 0.625$) and particularly with the AMO ($r_{O(50)} = 0.824$) (see auxiliary material for a discussion on statistical significance). This indicates that the simulated dynamical variability of the global climate, in the absence of external perturbations, is essentially captured by multidecadal recurrent atmosphere-ocean processes of which the PDO and the AMO are both regional manifestations.

[11] Multidecadal fluctuations appear also particularly strong in simulation S, i.e., solar forcing could naturally enhance such internal climate variability. However, the solar forcing considered here modulates the GST only moderately: Linear regression analysis indicates that TSI lag(0) contribution to GST variations is 0.07 $KW^{-1}m^2$ for simulation S (the maximum is 0.09 $KW^{-1}m^2$ for lag 55–56 years, therefore suggesting existence of a delayed response

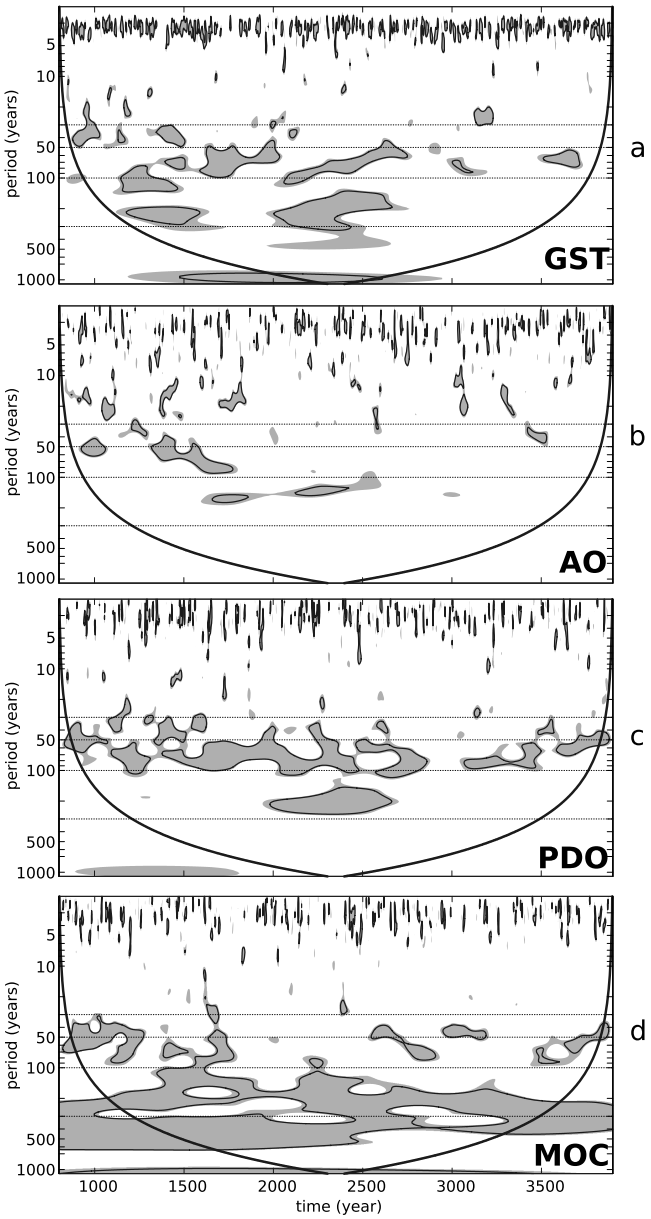

Figure 2. Wavelet spectra (a) of the annual Global Surface Temperature (GST), (b) of the winter Arctic Oscillation (AO), (c) of the winter Pacific Decadal Oscillation (PDO) and (d) of the annual Atlantic Meridional Overturning Circulation (MOC) for the full-length (3100 years) of simulation C (see Table 1 for details). Analysis and plot criteria as for Figure 1.

(Figure S4)). Multidecadal-to-centennial GST variations induced by TSI changes alone like the one considered here cannot alter remarkably the GST signal simulated by purely internal dynamics, and concur only for about half of the multidecadal-to-centennial GST variability as obtained in all forcing simulations (see Table 1). The regression coefficients between TSI and GST are higher for the E1-E5 ensemble (0.15 ± 0.03 $KW^{-1}m^2$ for the period 800–2005 and 0.12 ± 0.06 $KW^{-1}m^2$ for the pre-industrial period only), but this may be a spurious result originating from the superposition of different external forcing factors acting on the same timescale. In particular, simulated strong volcanic events (SVE) can induce very large and short-lived dynamical perturbations in the atmosphere [*Robock*, 2000] and also affect deep oceanic processes (see the MOC statistics in Table 1). Owing particularly to the inertia in oceanic recovery from large perturbations [*Stenchikov et al.*, 2009], SVE clusters can leave detectable traces on GST over decadal and larger timescales (Figure S4): The quasi-regular interval of occurrence of SVE clusters during the last millennium (about two hundred years) coincides with a prominent timescale characterizing TSI variability (Figures S5 and S6). Therefore, external forcing factors, acting together, have indeed left their imprint on simulated GST signals at centennial and longer timescales while overwhelming those, purely internal, at multidecadal-to-centennial timescales.

[12] We note also that, for both solar and volcanic forcing, correlations of external forcings with multidecadal patterns of AO, PDO and MOC are generally weak (Table S1), i.e., a robust agreement between individual forcing signals and simulated climate anomalies is rarely diagnosed.

[13] Figure 3 illustrates the multidecadal patterns of GST, MOC, PDO and AO simulated by the E1-E5 ensemble, further showing how the correlation among them varies throughout the integration time. An interesting aspect is that the ensemble standard deviations vary strongly over time, both for the individual time series and their cross-correlations. Thus, different time intervals exhibit different degrees of coherency in the behavior of the simulated climate, a feature which is anyway detectable also in simulation C (Figure S7). An apparent feature of GST is that ensemble standard deviations are small when the simulated climate evolution is predominantly determined by the imposed external forcing like, e.g., the SVE clusters in the mid 13th, 15th, and early 19th centuries and anthropogenic greenhouse gases in the 20th century. We note also that, generally, major transients in the correlations among GST, MOC, PDO and AO do not occur at the same time. For instance, transients in the MOC-AO and PDO-AO correlation are observed around AD 1200, while transients in the GST-MOC and GST-PDO correlation are observed around AD 1300. It appears thus that simulated climate fluctuations strongly depend upon how the various processes characterizing internal climate variability are affected by external forcings. Intriguingly, however, all runs performed including orbital forcing and anthropogenic aerosol and greenhouse gas (GHG) emissions show an almost monotonic increase in GST during the last 100 years or so, an increase which, while not evident in the winter PDO and AO, emerges also in the MOC. However, after a strong quasi-centennial positive anomaly, the MOC trend rapidly reverses (Figure S8), and the MOC further weakens after AD 2005 in the continuation of the runs with increasing GHG concentrations (not shown). Note that a similar strengthening of the simulated MOC in the early 20th Century was observed in the all-forcing simulations of *Tett et al.* [2007]. The details of the MOC response in our all-forcing experiments are presently subject of another study. First results indicate a complex response to regionally different temperature trends in the 19th century rather than a direct relation with GST. We also note that in simulations E1-E5 the MOC features energetic fluctuations at periodicities above O(100 years) (Figure S9), which are associated to a ~9% stronger pre-industrial MOC variability than in simulation C (see Table 1), i.e., in our simulations externally-

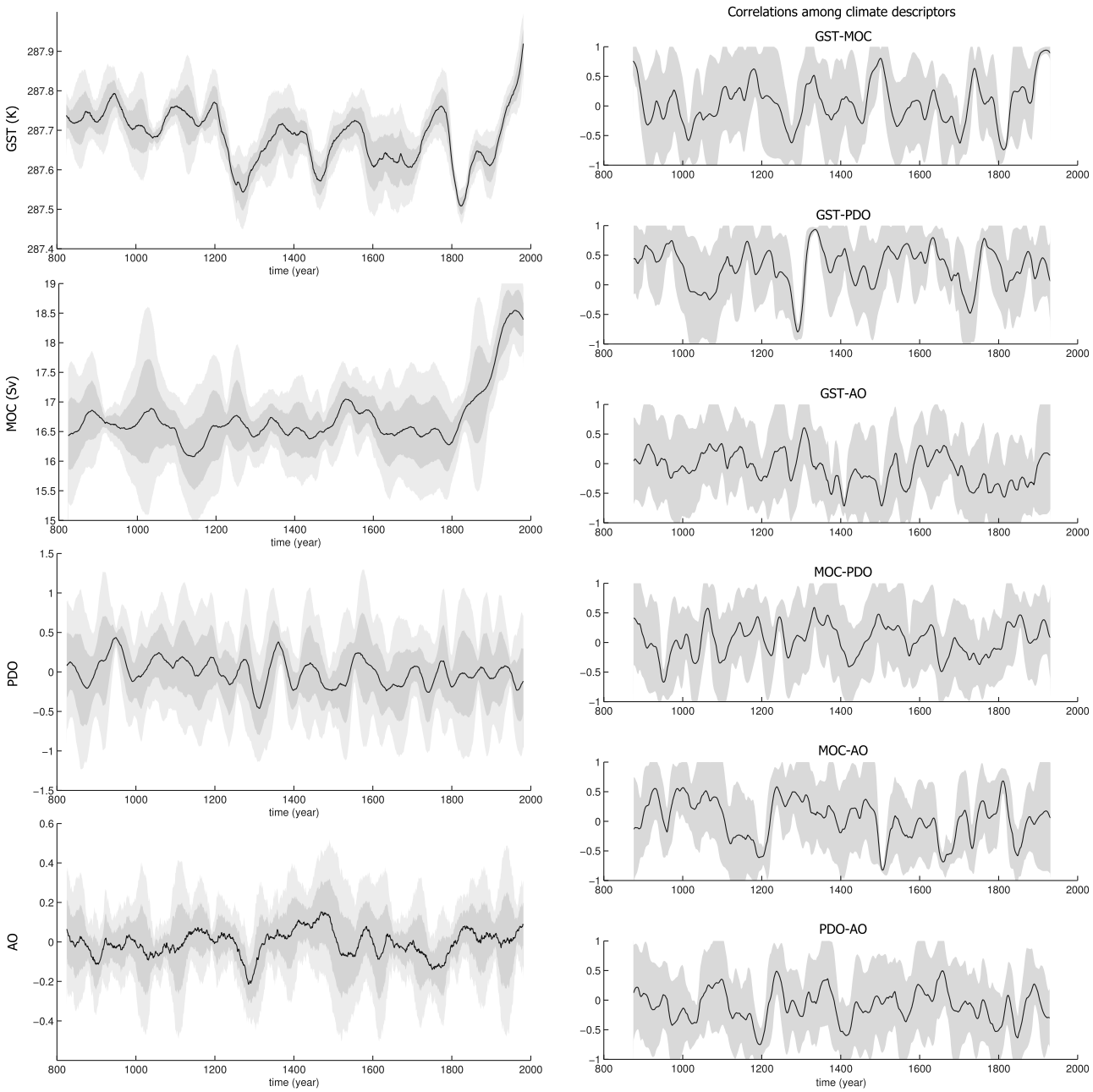

Figure 3. (left) Temporal evolution of multidecadal (O(50 years), see auxiliary material) Global Surface Temperature (GST), Atlantic Meridional Overturning Circulation (MOC), winter Pacific Decadal Oscillation (PDO) and winter Arctic Oscillation (AO) for the period AD 800–2005 as determined by the all forcing simulations ensemble (E1-E5 (see Table 1)). Black lines illustrate the ensemble average; dark (light) gray areas individuate one (two) standard deviations. (right) 51-year moving-window correlations among multidecadal GST, MOC, PDO and AO. Black lines illustrate the ensemble correlation average; gray areas individuate the ensemble one standard deviation.

forced variability enhances natural, internal modes of variability of deep oceanic processes.

[14] One key point for understanding the PDO-GST coupled variability seems the tendency of the PDO to maintain its predominant fluctuations around the multidecadal band also in the forced simulations (Figure S10), although with a loss of energy with respect to that expressed in an unperturbed climate system (Table S2). This feature points at the winter PDO as being a natural mode of climate variability which tends to be more resilient toward external perturbations than GST.

4. Conclusions

[15] The varying magnitude and irregular appearance of multidecadal-to-centennial climate signals thus seem to be a general feature of the dynamics of both observed and simulated climate systems. Simulated atmosphere-ocean pro-

cesses shape strongly the multidecadal evolution of GST in an unperturbed climate system. However, when external forcings are considered multidecadal GST fluctuations can be overwhelmed by centennial fluctuations and strongly distorted due to nonlinearities originated by different responses of internal climate processes to external perturbations. The relative importance of internal and externally-driven variability and their possible interference certainly adds complexity to the predictability of climate at decadal to multidecadal timescales.

[16] **Acknowledgments.** This work has been carried out as part of the MPI-M Integrated Project/*Millennium*/and contributes to the EU Integrated Project Thermohaline Overturning—At Risk? (THOR). A portion of this study has been supported by the ENIGMA project of the Max Planck Society (D. Z.). We thank Wolfgang Müller for the helpful comments and discussion.

References

Crespin, E., H. Goosse, T. Fichefet, and M. E. Mann (2009), The 15th century Arctic warming in coupled model simulations with data assimilation, *Clim. Past*, *5*, 389–401, doi:10.5194/cp-5-389-2009.

Gerber, S., et al. (2003), Constraining temperature variations over the last millennium by comparing simulated and observed atmospheric CO_2, *Clim. Dyn.*, *20*, 281–299.

Goosse, H., H. Renssen, A. Timmermann, and R. S. Bradley (2005), Internal and forced climate variability during the last millennium: A model-data comparison using ensemble simulations, *Quat. Sci. Rev.*, *24*, 1345–1360, doi:10.1016/j.quascirev.2004.12.009.

Jungclaus, J. H., et al. (2006), Ocean circulation and tropical variability in the coupled model ECHAM5/MPI-OM, *J. Clim.*, *19*, 3952–3972, doi:10.1175/JCLI3827.1.

Jungclaus, J. H., et al. (2010), Climate and carbon-cycle variability over the last millennium, *Clim. Past Discuss.*, *6*, 1009–1044, doi:10.5194/cpd-6-1009-2010.

Lawson, M. P., R. C. Balling, and A. J. Peters (1981), Spatial analysis of secular temperature fluctuations, *J. Clim.*, *1*, 325–332, doi:10.1002/joc.3370010405.

Mantua, N. J., S. R. Hare, Y. Zhang, J. M. Wallace, and R. C. A. Francis (1997), Pacific decadal climate oscillation with impacts on salmon, *Bull. Am. Meteorol. Soc.*, *78*, 1069–1079, doi:10.1175/1520-0477(1997)078<1069:APICOW>2.0.CO;2.

Parker, D. E., T. P. Legg, and C. K. Folland (1992), A new daily central England temperature series, 1772–1991, *Int. J. Climatol.*, *12*, 317–342, doi:10.1002/joc.3370120402.

Polyakov, I. V., et al. (2005), Multidecadal variability of North Atlantic temperature and salinity during the twentieth century, *J. Clim.*, *18*, 4562–4581, doi:10.1175/JCLI3548.1.

Pongratz, J., T. Raddatz, C. H. Reick, E. Esch, and M. Claussen (2009), Radiative forcing from anthropogenic land cover change since A.D. 800, *Geophys. Res. Lett.*, *36*, L02709, doi:10.1029/2008GL036394.

Robock, A. (2000), Volcanic eruptions and climate, *Rev. Geophys.*, *38*, 191– 219, doi:10.1029/1998RG000054.

Roeckner, E., et al. (2003), The atmospheric general circulation model ECHAM5. Part I: Model description, *Max Planck Inst. Meteorol. Rep. 349*, 127 pp., Hamburg, Germany.

Saenger, C., et al. (2009), Surface temperature trends and variability in the low-latitude North Atlantic since 1552, *Nat. Geosci.*, *2*, 492–495, doi:10.1038/ngeo552.

Shindell, D. T., and G. A. Schmidt (2003), Volcanic and solar forcing of climate change during the Preindustrial Era, *J. Clim.*, *16*, 4094–4107, doi:10.1175/1520-0442(2003)016<4094:VASFOC>2.0.CO;2.

Shindell, D. T., G. A. Schmidt, M. E. Mann, D. Rind, and A. Waple (2001), Solar forcing of regional climate change during the Maunder Minimum, *Science*, *294*, 2149–2152, doi:10.1126/science.1064363.

Stenchikov, G., et al. (2009), Volcanic signals in oceans, *J. Geophys. Res.*, *114*, D16104, doi:10.1029/2008JD011673.

Tett, S. F. B., et al. (2007), The impact of natural and anthropogenic forcings on climate and hydrology since 1550, *Clim. Dyn.*, *28*, 3–34, doi:10.1007/s00382-006-0165-1.

Thompson, D. W. J., and J. M. Wallace (1998), The Arctic Oscillation signature in the wintertime geopotential height and temperature fields, *Geophys. Res. Lett.*, *25*, 1297– 1300, doi:10.1029/98GL00950.

Trouet, V., et al. (2009), Persistent positive North Atlantic Oscillation mode dominated the medieval climate anomaly, *Science*, *324*, 78–80, doi:10.1126/science.1166349.

Zhang, R., T. L. Delworth, and I. M. Held (2007), Can the Atlantic Ocean drive the observed multidecadal variability in Northern Hemisphere mean temperature?, *Geophys. Res. Lett.*, *34*, L02709, doi:10.1029/2006GL028683.

J. H. Jungclaus and D. Zanchettin, Ocean in the Earth System Department, Max-Planck-Institute for Meteorology, Bundesstr. 53, D-20146 Hamburg, Germany. (davide.zanchettin@zmaw.de)

A. Rubino, Department of Environmental Sciences, University of Venice, Calle Larga Santa Marta, Dordosuro 2137, I-30123 Venice, Italy.